Production of isolated photons with jets in deep inelastic *ep* scattering at the ZEUS detector

Oleg Kuprash for the ZEUS collaboration

DESY, Notkestraße 85, 22607 Hamburg, Germany

DOI: `http://dx.doi.org/10.3204/DESY-PROC-2012-02/44`

Inclusive cross sections for the production of isolated photons accompanied by jets have been measured in neutral current deep inelastic scattering, for virtualities of the exchanged boson in the range $10 < Q^2 < 350\,\mathrm{GeV}^2$. The cross sections are compared to fixed-order perturbative QCD calculations and to the calculations based on k_T factorisation approach.

1 Introduction

This report presents measurements of isolated photons accompanied by jets in neutral current (NC) deep inelastic scattering (DIS) [1] performed with the ZEUS detector.

Isolated photons are photons emitted directly by quarks or leptons that take part in a hard scattering process. Photons emitted by leptons are called LL-photons, by quark - QQ-photons respectively. Example diagrams of these different processes are shown on Figure 1. Events with isolated photons provide a clean test of QCD since such photons do not undergo the hadronisation process and arrive in the detector unchanged after their production. The requirement for an accompanying jet enhances the QQ component of the cross section relative to LL and provides a test of perturbative QCD with two hard scales.

Figure 1: LL (left) and QQ (right) mechanisms of isolated photon production

2 Event Selection and extraction of the signal

The measurements are based on e^+p and e^-p data taken at HERA with integrated luminosities of $134\,\mathrm{pb}^{-1}$ and $198\,\mathrm{pb}^{-1}$, respectively. Events were selected by requiring a scattered-electron candidate with the polar angle $\theta^e > 140^\circ$ and energy $E^e > 10\,\mathrm{GeV}$. The kinematic quantity Q^2 was reconstructed from the scattered electron as $Q^2 = -(k - k')^2$, where k (k') is the four-momentum of the incoming (outgoing) lepton. The kinematic region $10 < Q^2 < 350\,\mathrm{GeV}^2$ was selected. To remove background from the photoproduction regime, where $Q^2 \approx 0\,\text{GeV}^2$, events were required to have $35 < E - p_Z < 65\,\text{GeV}$. Here $E - p_Z = \sum_i E_i(1 - \cos\theta_i)$, E_i is the energy deposited in i-th calorimeter cell, θ_i is its polar angle and the sum runs over all cells. A set of further cleaning cuts was applied.

The photon candidate, which is measured as a cluster of cells with signals in the calorimeter (CAL), was required to have a transverse energy in the range $4 < E_T^\gamma < 15\,\text{GeV}$. In order to measure well-understood shower shapes in the calorimeter, the photon was required to be recorded in the barrel section, with pseudorapidity in the range $-0.7 < \eta^\gamma < 0.9$. To reduce the background from neutral mesons, isolation criteria were applied: there should not be any track with momentum greater than 250 MeV within a cone of $\Delta R = 0.2$ around the photon candidate, where $\Delta R = \sqrt{(\Delta\phi)^2 + (\Delta\eta)^2}$ is the distance in the pseudorapidity-azimuthal plane. It was required that at least 90% of the measured photon energy should be deposited in the electromagnetic sections of the CAL. In order to reduce the fraction of events with quark-to-photon fragmenation (which is not discussed in this report), the ratio of the photon energy to the energy of the jet containing the photon was required to be greater than 0.9, thereby isolating the photon.

Jets were selected with transverse energies $E_T^{\text{jet}} > 2.5\,\text{GeV}$ and pseudorapidities in the range $-1.5 < \eta^{\text{jet}} < 1.8$. The jets were clustered using the k_T algorithm in the longitudinally invariant inclusive mode as implemented in the HEPFORGE KTJET package [2].

For the signal extraction of isolated photons a shower shape technique was utilised. The variable $\langle \delta Z \rangle = \sum_i |Z_i - Z_{\text{cluster}}|/(w_{\text{cell}} \sum_i E_i)$ was used to describe the shower shape; its distribution is shown in Figure 2. Here Z_i is the Z position of the centre of the $i-$th cell, Z_{cluster} is the Z position of the centre of the CAL cluster where the photon candidate deposited its energy, w_{cell} is the cell width in the Z direction, and E_i is the energy deposited in the cell. The sum runs over the barrel CAL cells of the cluster.

Separate Monte Carlo samples were used for the simulation of the LL- and QQ-photon production. The $\langle \delta Z \rangle$ distribution in data was fitted by the sum of the Monte Carlo distributions in the range $0 < \langle \delta Z \rangle < 0.8$.

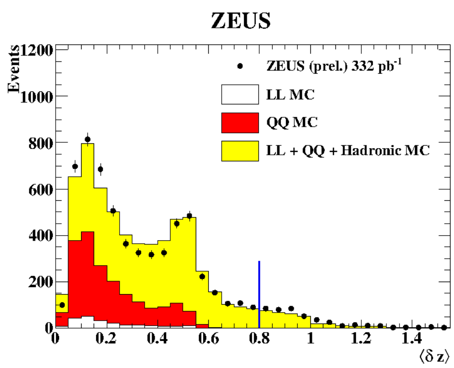

Figure 2: Distribution of $\langle \delta Z \rangle$

3 Theoretical predictions

The results are compared to new theoretical calculations. The GKS predictions [3] are fixed-order NLO calculations at order $\alpha^3\alpha_s$ in the electromagnetic and strong couplings. They take into account both LL and QQ contributions as well as the LQ interference term. The LQ interference term gives an effect of $\approx 3\%$ on the cross sections and this effect is reduced to $\approx 1\%$ when e^+p and e^-p data are combined since the sign of the term is different for e^+p and e^-p. The calculations were obtained using the HERAPDF1.0 [4] parameterisations for the proton PDFs with the factorisation and renormalisation scales set to $\mu_F = \mu_R = \sqrt{Q^2 + (p_T^{\rm jet})^2}$. The uncertainty due to the choice of the renormalisation and factorisation scales, which is the largest source of the overall theoretical uncertainty, were evaluated by scaling μ_R and μ_F by a factor 2 up and down independently. The total uncertainty on the integrated cross section is about 5% rising to approximately $\pm 10\%$ at large negative jet pseudorapidities.

The BLZ predictions [5] are made in the framework of the QCD k_T factorisation approach based on the off-shell partonic amplitude $eq^\star \to e\gamma q$. Photon radiation from the quarks as well as from the leptons are taken into account. Unintegrated proton parton densities are used in the KMR model. Uncertainties are mainly due to the procedure for the setting of the accompanying jet rapidity and are up to 20%.

4 Results

The phase space of the measurements was defined by $10 < Q^2 < 350\,{\rm GeV}^2$; the selected events were required to have a well reconstructed electron with energy $E^e > 10\,{\rm GeV}$ and scattering angle $\theta > 140^\circ$. The photon was required to have transverse energy in the range $4 < E_T^\gamma < 15\,{\rm GeV}$ and pseudorapidity $-0.7 < \eta^\gamma < 0.9$. If the photon belongs to a jet, photon energy must be greater than $0.9E^{\rm jet\,containing\,\gamma}$. The transverse energy of the accompanying jet was greater than 2.5 GeV and its pseudorapidity was in range $-1.5 < \eta^{\rm jet} < 1.8$. The jets were reconstructed using the k_T clustering algorithm in the $E-$scheme in the longitudinally invariant inclusive mode with the R parameter set to 1.0.

In Figure 3 differential cross sections as function of E_T^γ, η^γ, Q^2, x, $E_T^{\rm jet}$ and $\eta^{\rm jet}$ are presented. For the QQ-events x is the fraction of the proton momentum carried by the incoming parton, x is defined as $Q^2/(2P(k-k'))$, where P is the four-momentum of the incoming proton.

Both theories provide a reasonable description of the data in shape, however the GKS theory agrees better with the cross sections as functions of jet variables. The GKS predictions systematically underestimate the data by typically 20% while the BLZ predictions overestimate them by about 20%.

The results indicate the necessity for further improved QCD calculations.

References

[1] H. Abramowicz *et al.* [ZEUS Collaboration], arXiv:1206.2270 [hep-ex].

[2] J. M. Butterworth, J. P. Couchman, B. E. Cox and B. M. Waugh, Comput. Phys. Commun. **153** (2003) 85 [hep-ph/0210022].

[3] A. Gehrmann-De Ridder, G. Kramer and H. Spiesberger, Nucl. Phys. B **578** (2000) 326 [hep-ph/0003082].

[4] F. D. Aaron *et al.* [H1 and ZEUS Collaboration], JHEP **1001** (2010) 109 [arXiv:0911.0884 [hep-ex]].

[5] S. P. Baranov, A. V. Lipatov and N. P. Zotov, Phys. Rev. D **81** (2010) 094034 [arXiv:1001.4782 [hep-ph]].

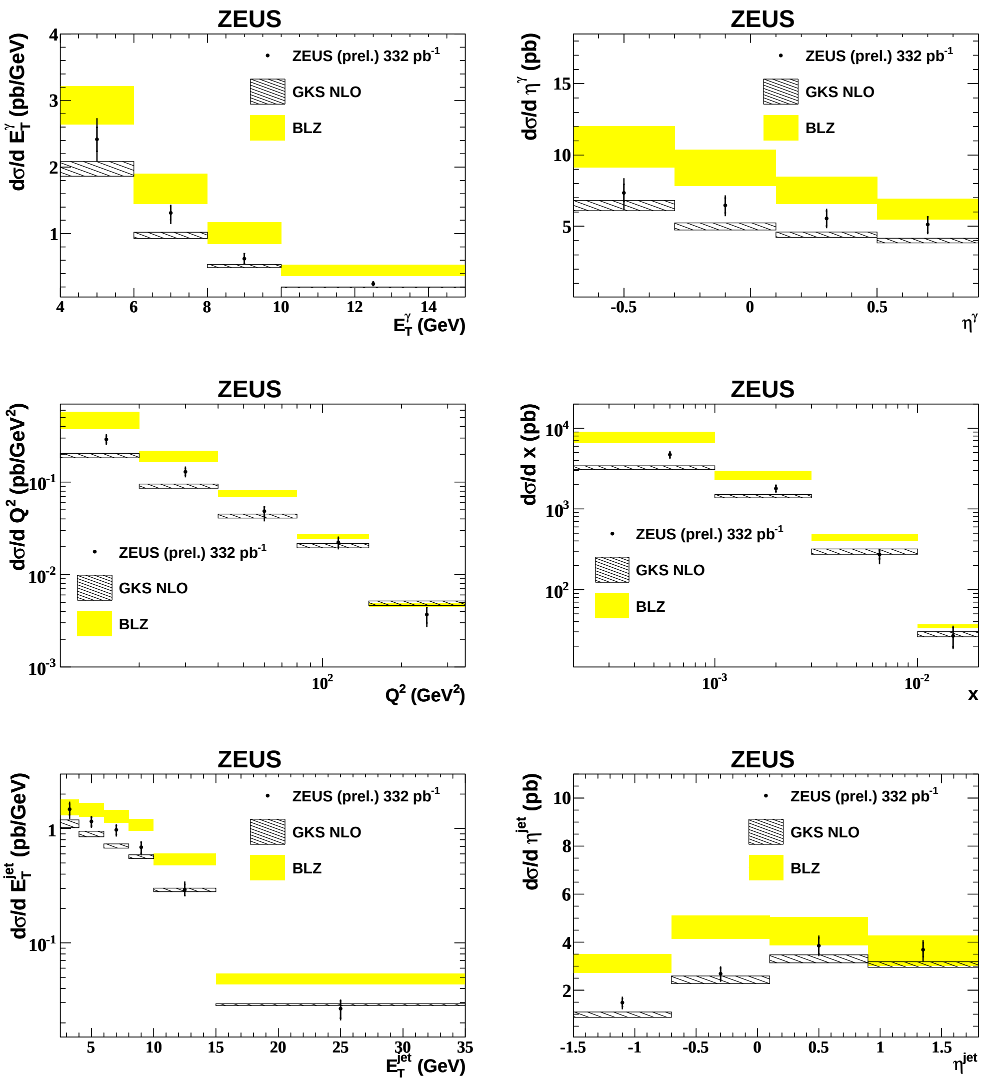

Figure 3: Differential cross sections as functions (from left to right, top to bottom) of the photon energy, the photon pseudorapidity, x, Q^2, the jet energy and the jet pseudorapidity